Correlative assessment of structural and photoelectrical properties of thermally evaporated CdSe thin films

K. Sarmah*, R. Sarma and H. L. Das
Department of Physics, Gauhati University, Guwahati-781014, India

Cadmium Selenide thin films of different thicknesses, (1530-2230Å) deposited by thermal evaporation on suitably cleaned glass substrates at different substrate temperatures (473-623K) are of polycrystalline nature having hexagonal structure. In gap type cell configuration of these films with thermally evaporated aluminium electrodes, the I-V characteristics are observed to be linear both under dark and monochromatic illuminations for low bias voltages, but show Poole-Frenkel type of conductivity for high bias voltages under the same illuminations. The values of lattice constant, grain size, microstrain and dislocation density of the deposited films are calculated and these are co-related with different photoelectrical parameters.

(Received February , 28, 2009; accepted May 5, 2009)

Keywords : CdSe thin film, Lattice constant, Grain size, Microstrain, Dislocation density

1. Introduction

CdSe is a binary II-VI semiconductor and among this group of semiconductor compounds, it is considered as an important material for the development of different optoelectronic devices [1,2,3] because of its high photosensitive nature and suitable intrinsic band gap [4]. In recent years special attention has been given to the investigation of optoelectronic properties of CdSe thin films in order to improve the performance of devices made of it and also for finding new applications [5,6]. For preparation of CdSe thin films, different growing methods have been used [7,8]. Physical vapour deposition in its variants is often used as it offers many possibilities to modify the deposition parameters and to obtain films with pre-determined structure and suitable photo-transport properties. Electrical and optical properties of semiconducting films are essential requirement for proper application in various optoelectronic devices. These properties of the films are sufficiently structure sensitive. Therefore appropriate structural characterization of the films is necessary. It may be noted that the structural parameters such as crystallinity, crystal phase, lattice constant, grain size etc are strongly dependent on the deposition conditions. The structure of thermally deposited CdSe thin films is likely to be governed by the degree of vacuum, rate of deposition, substrate temperature, film thickness etc. An experimental study has been undertaken in order to structurally characterize thermally evaporated CdSe thin films and to study their photoelectrical behaviour. In this paper some correlative results of different structural parameters with few photoelectrical attributes has been reported.

2. Experimental

Thin films of CdSe of different thickness, t, (1530-2230Å) were deposited at different substrate temperatures, T_s (473-623K), on chemically and ultrasonically cleaned glass substrates at a vacuum better than 10^{-5} torr. The prepared films were annealed in vacuum at elevated temperature and hereafter stored in dry air for a definite period of time. Pure (99.999%) bulk CdSe sample was used as the source material. Thin tantalum boats of proper size and shape were used as the source heater. A suitably designed and assembled multiple beam interferometer was used to measure the thickness of the films with an accuracy of ±15Å. X-ray diffractogram (XRD) of CdSe thin films were taken by using Philips X-ray diffractometer (Philips X'Pert Pro) with CuKα radiations of wavelength 1.54Å. In the annealed films, used for photoelectrical studies, high purity aluminium electrodes were vacuum evaporated to obtain a gap type cell configuration of 10mm x 7mm geometry. An ECIL electrometer amplifier of input impedance of $10^{14}\Omega$ (and higher) was used to measure dark and photocurrents. To apply dc bias, a series of highly stable dry cells of emf 9 volt each was used. For white light illuminations tungsten halogen projector lamp of 250 watt, operating at maximum voltage 24V, was used. A set of C-Z metal interference filters of different wavelengths starting from 600 nm to 900 nm was used to obtain monochromatic radiations. The intensities were measured by using a highly sensitive APLAB luxmeter. The entire experimental set up including the observer was housed in a suitably fabricated Faraday cage in order to avoid pick-up noises.

Surface morphology of the CdSe films was investigated by using scanning electron microscope (SEM) with an accelerating potential of 18kV and the quantitative analysis was carried out with the help of EDAX (Wavelength dispersive X-ray analyzer) attached with the SEM

3. Results and discussions

3.1 Structural parameters

3.1.1 Determination of lattice constant

The lattice parameter, a, for cubic phase structure [hkl] is determined by the relation

$$d_{hkl} = a/(h^2+k^2+l^2)^{1/2} \qquad (1)$$

where $N = h^2+k^2+l^2$ is a number. Observing the distribution of N values, the type of the cubic lattice may be determined [9].
From the Bragg's law,

$$\lambda = 2a \, \mathrm{Sin}\theta \, / \, (h^2+k^2+l^2)^{1/2}$$

$$\mathrm{Sin}^2\theta = (\lambda^2/4a^2)(h^2+k^2+l^2) = \lambda^2 N / 4a^2 \qquad (2)$$

For hexagonal crystals; the lattice constants, a, and, c, are evaluated from the following relations

$$1/d^2 = [(4/3)\{(h^2+hk+k^2)/a^2\}] + (l^2/c^2) \quad (3)$$

From Bragg's law

$$Sin^2\theta = [(\lambda^2/3)\{(h^2+hk+k^2)/a^2\}] + (\lambda^2 l^2/4c^2) \quad (4)$$

According to Vegards law, the lattice parameters of hexagonal unit cell are nearly related to cubic lattice parameters of same material by [10]

$$a_{hex} = (1/2)^{1/2} a_{cubic} \qquad c_{hex} = (4/3)^{1/2} a_{cubic} \quad (5)$$

Hence for 'ideal' Wurtzite lattice, the relation [11] between the two lattice parameters is

$$c_{hex} = (1.633) a_{hex} \quad (6)$$

which can be used for the calculation of lattice parameters of CdSe thin films.

3.1.2 Grain Size

The grain size (D_{hkl}) for the thermally evaporated CdSe thin films are evaluated for the preferred planes [hkl] using the Scherrer formula [12]

$$D_{hkl} = k\lambda / \beta_{2\theta}\cos\theta \quad (7)$$

with k = 0.94, where θ is the Bragg's angle, λ is the wavelength of X-rays used, $\beta_{2\theta}$ is the width of the peak at the half of the maximum peak intensity.

3.1.3 Average strain

The origin of strain is related to lattice 'misfit' which in turn depends upon the growing conditions of the films. The microstrain (ε) developed in the thin films can be calculated from the relation [13]

$$\varepsilon = (\beta_{2\theta}\cot\theta) / 4 \quad (8)$$

where θ and $\beta_{2\theta}$ has their usual significances.

3.1.4 Dislocation Density

Dislocations are an imperfection in a crystal associated with misregistry of the lattice in one part of the crystal with respect to another part. Unlike vacancies and interstitial atoms, dislocations are not equilibrium imperfections, i.e. thermodynamic considerations are insufficient to account for their existence in the observed densities. In fact, the growth mechanism involving dislocation is a matter of importance. In the present study, the

dislocation density of thin films is estimated by using the Williamson and Smallman's relation [14]

$$\delta = n / D^2 \quad (9)$$

where n is a factor, which equals unity giving minimum dislocation density and D is the grain size.

3.2 Structural characterization

The X-ray diffraction profiles of CdSe thin films of different thicknesses, t, (1530-2230Å) reveal that films grown at room temperature are amorphous (Fig 1) and those grown at elevated substrate temperatures, T_s (473-623K) are polycrystalline having hexagonal ZnS type structure (Figs 2 & 3). This is confirmed by comparing the observed 'd' values of the XRD patterns of the films with the standard 'd' values of JCPDS X-ray powder file data [15]. In these films [002] plane is very clear and abundant. However small percentage of orientations of [110], [112] & [100] planes are also observed depending upon T_s of deposition. For the film deposited at 573K diffracted intensity from [100] and [110] is comparable to the corresponding intensity for [002] plane. The dominance of [002] hexagonal reflection indicates that the preferential growth of crystallite is in this particular direction. The broad hump that is observed in the background of XRD is due to the amorphous glass substrate and also possibly due to some amorphous phase present in the CdSe thin film.

Different structural parameters of the CdSe thin films having different, t as well as T_s are calculated by using relevant formulae and are systematically presented in tables 1 and 2. The data of the tables show variations in the structural parameters of the films with deposition temperature, film thickness and also along different orientations.

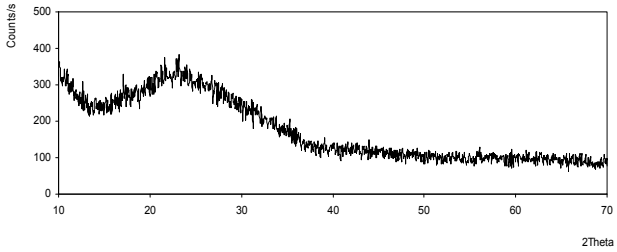

Figure 1 *X-ray diffraction pattern of a CdSe thin film of thickness t = 2000Å and grown at room temperature.*

With increase of T_s the crystallinity of the films is found to be improved substantially. At higher T_s in the formation process of the films, ad-atoms possess greater mobility along direction parallel to the substrate surface, which thus contribute to improvement of the crystallization processes.

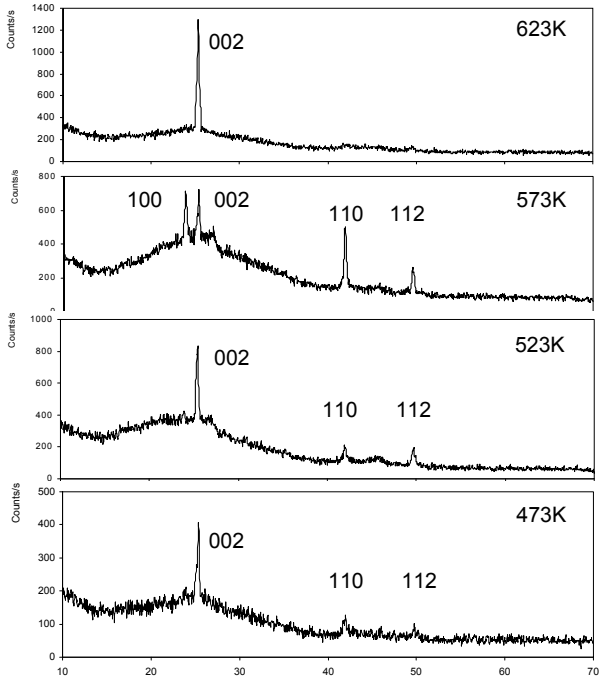

Figure 2 *X-ray diffraction patterns of CdSe thin films of thickness t = 2000Å and deposited at different T_S = 623K, 573K, 523K and 473K respectively.*

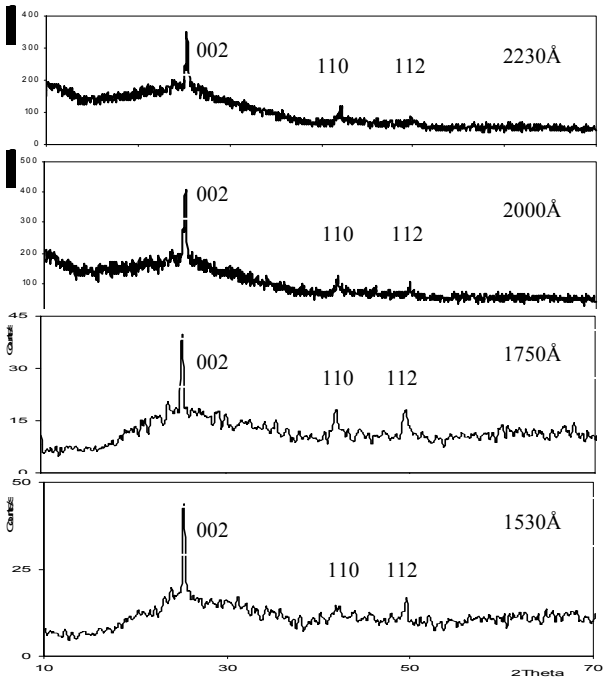

Figure 3 *X-ray diffraction patterns of CdSe thin films of thickness t = 2230Å, 2000Å, 1750Å and 1530Å respectively and deposited at the same T_S = 473K.*

Table 1 *Calculated values of the structural parameters of CdSe thin films of same t = 2000Å and deposited at different T_s*

T_s (K)	hkl	a (Å)	c (Å)	D_{hkl} (Å)	ε in 10^{-3}	δ in 10^{11} cm^{-2}
623	002	4.298	7.011	350	4.70	0.81
573	100	4.307	7.025	268	6.52	1.39
	002	4.310	7.029	308	5.35	1.05
	110	4.306	7.024	295	3.42	1.14
	112	4.306	7.023	253	3.40	1.56
523	002	4.296	7.006	283	5.80	1.24
	110	4.297	7.008	301	3.34	1.10
	112	4.301	7.015	201	4.26	2.47
473	002	4.303	7.018	280	5.90	1.27
	110	4.297	7.008	253	3.97	1.56
	112	4.293	7.003	221	4.17	2.04

Table 2 *Calculated values of structural parameters of CdSe thin films of different t and deposited at same T_s = 473K.*

t (Å)	hkl	a (Å)	c (Å)	D_{hkl} (Å)	ε in 10^{-3}	δ in 10^{11} cm^{-2}
2230	002	4.301	7.016	323	5.10	0.95
	110	4.291	6.999	341	2.95	0.85
	112	4.290	6.997	326	2.63	0.94
2000	002	4.303	7.018	280	5.90	1.27
	110	4.297	7.008	253	3.97	1.56
	112	4.293	7.003	221	4.17	2.04
1750	002	4.323	7.052	275	6.20	1.32
	110	4.301	7.015	185	5.46	2.92
	112	4.312	7.032	145	5.95	4.75
1530	002	4.320	7.046	171	9.67	3.41
	110	4.297	7.009	167	6.01	3.58
	112	4.314	7.037	228	3.78	1.92

4. I-V characteristics

Varition of dark current, I_D, with applied bias voltage for the CdSe thin films are found to be linear (ohmic) within the applied bias range (-108V) to (+108V). For the low bias voltages of both polarities, current under illumination (I_L) varies linearly with bias and in high voltage range I_L increases nonlinearly with the applied bias. In these regions when $\ln J_{ph}$ (J_{ph} is the photocurrent density, photocurrent $I_{ph}=I_L-I_D$) is plotted against $F^{1/2}$ (F being the field corresponding to the applied bias) the plots [Figs 4(a,b)] are found to be linear in high field regions and non-linear in low fields.

It is apparent from the $\ln J_{ph}$ verses $F^{1/2}$ characteristics depicted in Figs 4(a,b) for different films, that the basic nature of the curves are similar apart from the numerical values, both in low and high field regions.

The linear nature in high field regions clearly indicates the predominance of Poole-Frenkel type of conduction mechanism at high fields. This type of conductivity mainly depends upon the grain boundary potentials, which may be modified by externally applied fields. The current density due to such type of conduction mechanism is given by [16]

$$J = J_o \exp (\beta_{PF} F^{1/2}/kT) \qquad (10)$$

where $\sigma_o F = J_o$ is the low field current density, β_{PF} is the Poole-Frenkel coefficient and other symbols have their usual significance. From the slopes

$$m = \beta_{PF} / kT \qquad (11)$$

of the $\ln J_{ph}$ versus $F^{1/2}$ plots the Poole-Frenkel coefficients are calculated which are found to be in the range (4.4 - 4.9) x 10^{-4} eV $V^{-1/2}$ $m^{1/2}$.

These values of experimental β_{PF} are higher than those predicted theoretically which suggest the existence of localized electric fields within the films having values higher than mean field F = V/d, where d is the electrode separation. Such localized fields may be present as a result of number of different effects; band bending in the region of the contacts due to the difference in work function between the metal and semiconductor is one possibility, while the different localized environments of individual trapping centers in the grain boundary regions of the film are unlikely to result in an exactly linear variation in potential on a microscopic scale and thus in a spatially constant electric field.

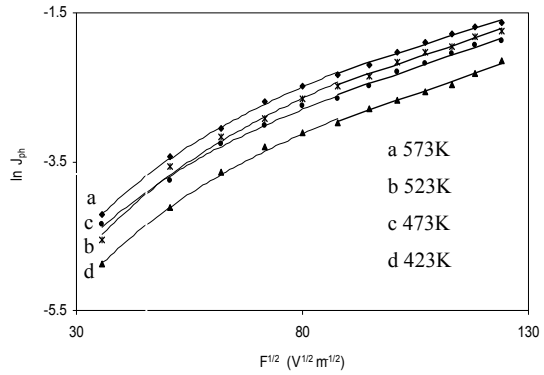

Figure 4(a) *$\ln J_{ph}$ verses $F^{1/2}$ of CdSe thin films of constant thickness, deposited at different T_s under constant monochromatic illumination of 725nm*

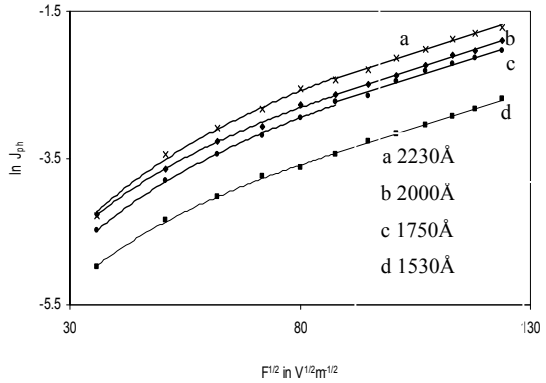

Figure 4(b) *$\ln J_{ph}$ verses $F^{1/2}$ of CdSe thin films of different thickness, deposited at constant elevated T_s , under constant monochromatic illumination of 725nm.*

As the average grain sizes in higher T_s grown films are higher (XRD patterns given in Figs 2 & 3), the corresponding average grain boundary potentials are lowered.

The Poole-Frenkel effect of field lowering of built-in potentials in the body of the thin films decreases in the films deposited at higher T_s.

5. Correlative assessments

In the present study the photoconductivity (σ_{ph}) of CdSe thin films is found to increase rapidly with grain size for the films deposited at different T_s and also for films of different t [Figs 5(a, b)]. XRD data show that films grown at higher T_s are essentially polycrystalline with higher grain size and the photoconductivity increases with reduction of grain boundary defect states.

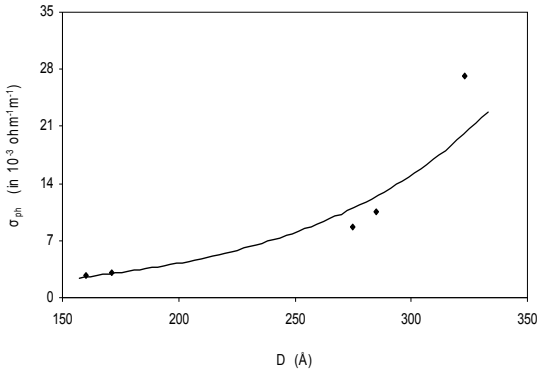

Figure 5(a) *Variation of σ_{ph} with D_{hkl} of CdSe thin films of constant t = 2000Å and grown at different elevated T_s*

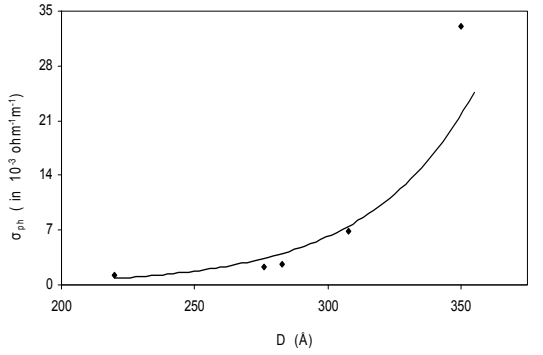

Figure 5(b) *Variation of σ_{ph} with D_{hkl} of CdSe films of different, t, grown at constant T_s = 473K*

Improvement of crystallinity of the films results in a decreasing nature of strain. That is films with lesser values of strain may be obtained by depositing the films at higher elevated temperature. From the plots of photoconductivity versus strain, [Figs 6(a, b)], it is observed photoconductivity (σ_{ph}) decreases with strain (ε).

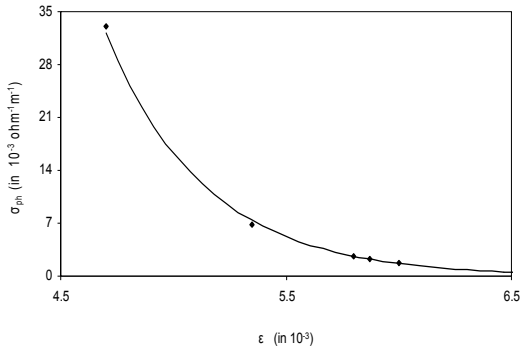

Figure 6(a) *Variation of σ_{ph} with ε of CdSe thin films of constant t = 2000Å grown at different elevated T_s*

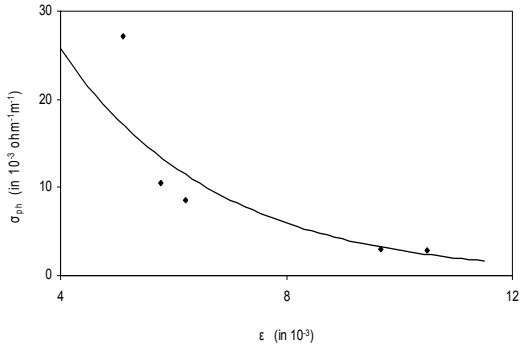

Figure 6(b) *Variation of σ_{ph} with ε of CdSe thin films of different, t, and grown at constant elevated T_s = 473K*

From the present analysis it is found that polycrystalline CdSe thin films are characterized by Poole-Frenkel type of conductivity and barrier modulated photoconductivity. Figs 7(a, b) show that Poole-Frenkel coefficient (β_{PF}) has a linear relationship with the grain size with a negative slope whereas plots of β_{PF} versus strain depicted in Figs 8(a, b) show that the coefficient increases with strain.

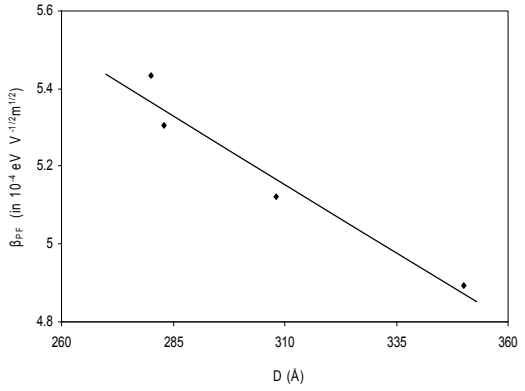

Figure 7(a) *Variation of β_{PF} with D_{hkl} of CdSe thin films of constant t = 2000Å and grown at different elevated T_s*

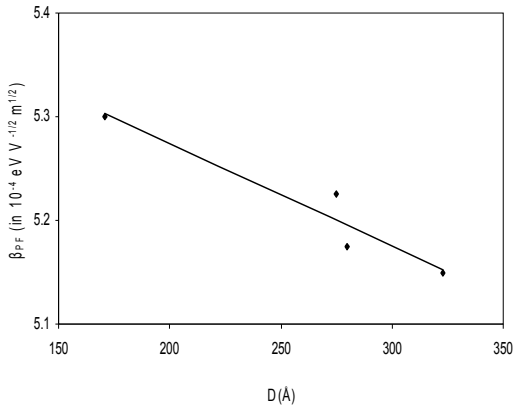

Figure 7(b) *Variation of β_{PF} with D_{hkl} of CdSe thin films of different, t, and grown at constant elevated T_s = 473K*

In the polycrystalline samples dislocated atoms occupy the regions near the grain boundaries. The effect due to the presence of dislocated atoms or molecules near grain boundary on the electronic structure and optical properties of polycrystalline semiconductor is mainly determined by (a) crystal structure distortions, (b) the presence of mechanical stresses due to structural defects, (c) internal electric fields arising as a result of screening of the charge near the grain boundary [17].

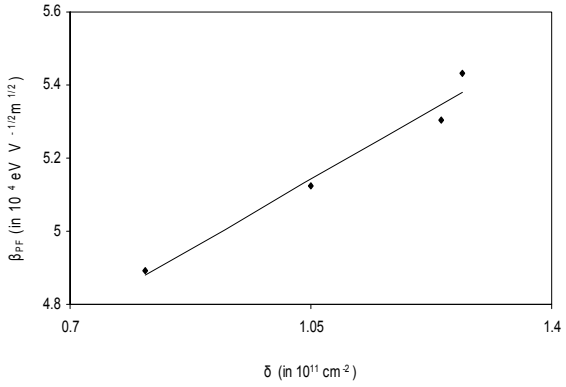

Figure 8(a) *Variation of β_{PF} with ε of CdSe thin films of constant t = 2000Å and grown at different elevated T_s*

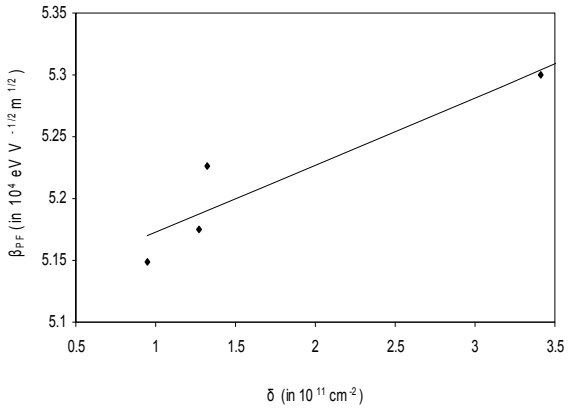

Figure 8(b) *Variation of β_{PF} with ε of CdSe thin films of different, t, and grown at constant T_s = 473K.*

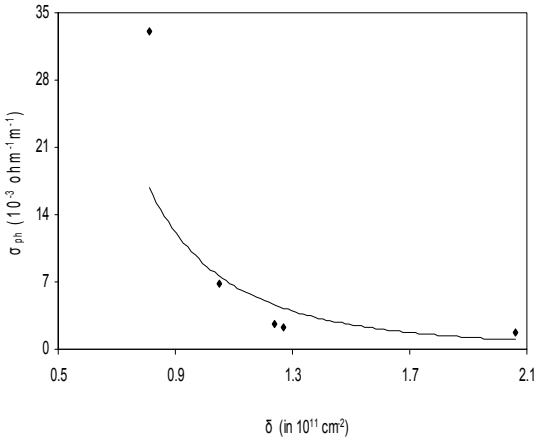

Figure 9(a) *Variation of σ_{ph} with δ of CdSe thin films of constant, t = 2000Å and grown at different elevated T_s*

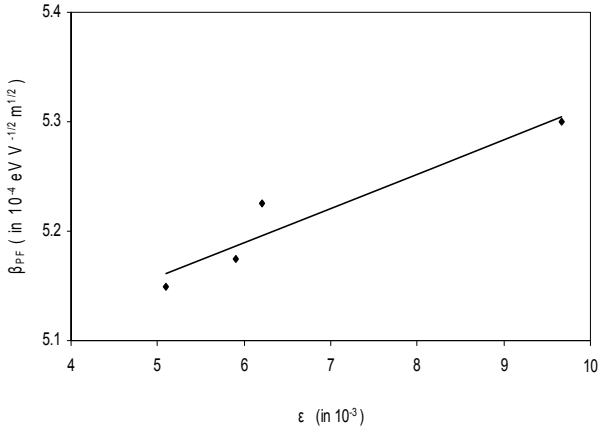

Figure 9(b) *Variation of σ_{ph} with δ of CdSe thin films of different, t, and grown at constant T_s = 473K.*

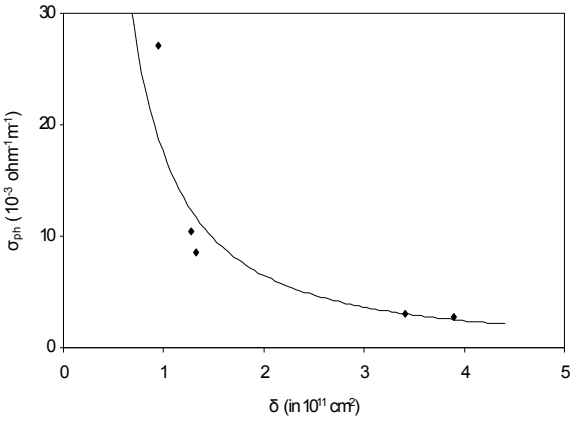

Figure 10(b) *Variation of β_{PF} with δ of CdSe thin films of different, t, and grown at constant elevated T_s = 473K*

Figs 9(a, b) show the plots of photoconductivity versus average dislocation density (δ). It is found that the photoconductivity of the films decreases exponentially with the dislocation density. Therefore it can be concluded that increase in the number of dislocation enhance the contribution of defects which in turn reduce the photoconductivity of the films. As already mentioned dislocation density has an inverse square variation with grain size. Figs 10(a, b) show that there is a linear variation of β_{PF} with dislocation density.

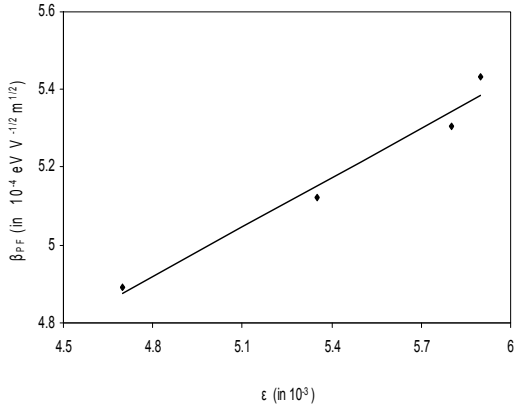

Figure 10(a) *Variation of β_{PF} with δ of CdSe thin films of constant t = 2000Å and grown at different elevated T_s*

6. Morphological Study

(a) Scanning Electron Microscope

The film morphology under SEM studies show that the films deposited at higher substrate temperatures (below 623K) are fairly uniform, polycrystalline and free from macroscopic defects like cracks or peeling. So for the photoelectrical observations the qualities of such grown films are quite suitable.

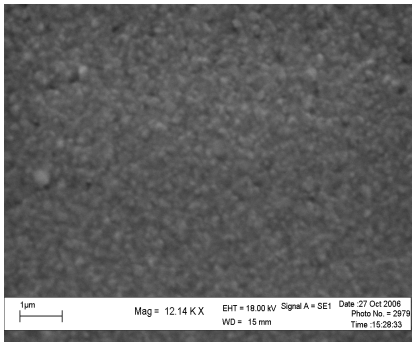

Figure 11(a) *SEM of a CdSe thin film (t = 2000Å, T_S = 473K) Magnification 12.14 KX*

(b) Quantitative Analysis

The quantitative analysis of CdSe films were carried out by using EDAX technique for 'as-deposited' CdSe thin films, at different points to study the stochiometry of the films. Fig 11(b) shows a typical EDAX pattern and details of relative analysis for a CdSe thin film.

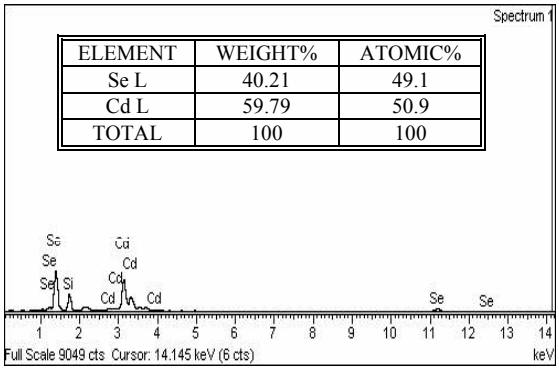

ELEMENT	WEIGHT%	ATOMIC%
Se L	40.21	49.1
Cd L	59.79	50.9
TOTAL	100	100

Figure 11(b) Typical EDAX pattern along with relative analysis of an 'as-deposited' CdSe thin film grown at elevated T_s .

The elemental analysis was carried out only for Cd and Se; the average atomic percentage of Cd:Se was 50.9:49.1, showing that the sample was slightly Se deficient. The Si peak that is observed in the EDAX pattern is due to the glass substrate used for deposition of CdSe thin films.

7. Conclusions

The CdSe films thermally deposited at room temperature are amorphous and those grown at higher T_s range 473K to 623K and thickness range 1530Å to 2230Å are polycrystalline in nature having hexagonal ZnS type structure. The most preferred orientations for CdSe thin film is along the hexagonal [002] direction. Orientations along [110], [112] and [100] directions are relatively in smaller percentage.

Dark conductivity of the films yields ohmic contacts with thermally evaporated aluminium electrodes and from the plots of J_{ph} verses $F^{1/2}$ of CdSe thin films it is observed that no space charge injection mechanism prevails in the sample and the photoconductivity

phenomenon is governed by Poole-Frenkel mechanism. The photoconductivity process in polycrystalline CdSe thin films is highly structure sensitive.

References

[1] C. Baban, G. G. Rusu and G. I. Rusu, J. Phys.: Condens Mater, **12,** 7687 (2000).
[2] P. K. Kalita, B. K. Sarma and H. L. Das, Bull. Mater. Sci. **26,** 613 (2003).
[3] K. C. Sathyalatha, S. Uthanna and P. Jayaramareddy, Thin Solid Films, **174,** 233 (1989)
[4] K. N. Shreekanthan, B. V. Rajendra, V. B. Kasturi and G. K. Shivakumar, Cryst. Res. Technol., **38,** 30 (2003)
[5] A. O. Oduor and R. D. Gould, Thin Solid Films, **317,** 409, (1998).
[6] U. Pal, D. Samanta, S. Ghorai and A. K. Chaudhuri , J. Appl. Phys. **74**(10)**,** 6368, (1993).
[7] R. B. Kale and C. D. Lokhande, Semicond. Sci. Technol. **20**(1), 1, (2005).
[8] C. Baban, G. I. Rusu and P. Prepelita, J. Optoele. & Adv. Mat., **7**(2), 817, (2005).
[9] I. H. Khan in Hand Book of Thin Film Technology (Eds) L. I. Maissel and R. Glang, Mc-Grow Hill Co., N.Y., Chap. 9,19, (1970).
[10] W. L. Roth in M. Aven and J. S. Prener (eds) Physics and Chemistry of II-VI Compounds, North-Holland Publishiong Co. Amstredam, 124, (1967).
[11] N. G. Dhere, N. R. Parikh and A. Ferreir, Thin Solid Films, **44**, 83, (1977).
[12] H. P. Klug and L. E. Alexander, X-ray Diffraction Procedures, John Willey and Sons, Inc New York, Chapter 9 512. (1954).
[13] S. Sen, S. K. Halder and S. P. Sen Gupta, J. Phys. Soc. Japan, **38**(6), 1641, (1975).
[14] D. P. Padiyan, A. Marikani and K. R. Murali, Mat. Chem. and Phys., **78**, 51, (2002).
[15] Powder Diffraction Data File, Joint Committee of Powder Diffraction Standard, International Center for Diffraction Data, USA Card No. 8-459, p143, (1984).
[16] J. G. Simmons in Hand Book of Thin Film Technology (eds) Maissel L I and Glang R, Mc Graw-Hill Book Company, N. Y., Chap 14, (1970).
[17] L. B. Freund and S. Suresh; Thin Film Materials - Stress, Defect Formation and Surface Evolution, Cambridge University Press, (2003).

* corresponding author: ks_guphys@rediffmail.com